

SUPPLEMENTARY INFORMATION

TITLE: VISSOR: A SOFTWARE PACKAGE FOR SPIKE SORTING OF NEURAL DATA.

Acronym: VISSOR (*Viability of Integrated Spike Sorting of Real Recordings*).

VISSOR Block Diagram (Figure S1):

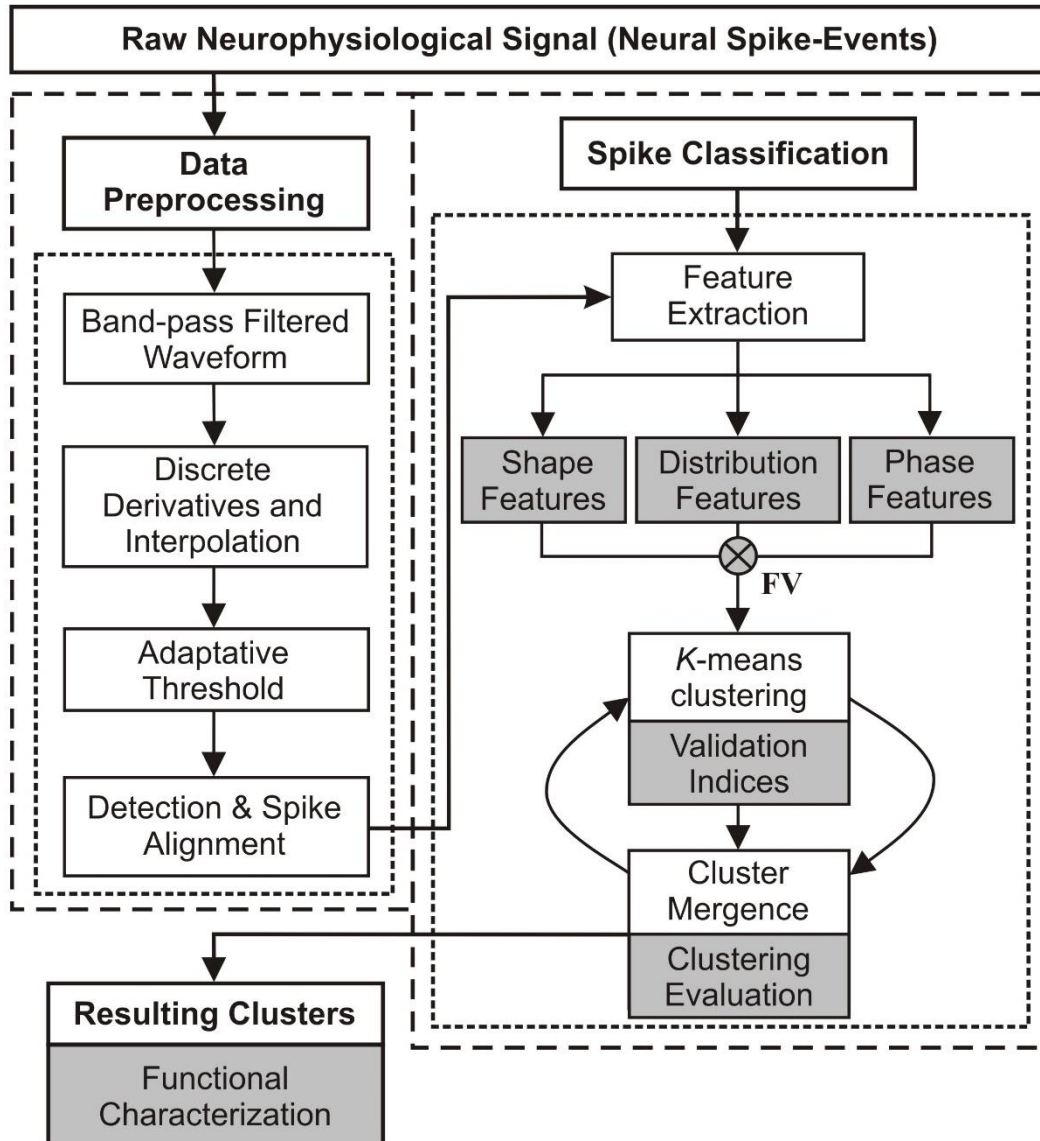


Figure S1. Overall structure of the proposed SS-SPDF method/algorithm. Step-by-step illustration of the spike-sorting process based on shape, phase, and distribution features, and *K*-means clustering with internal validation indices. White blocks represent the common steps of a spike-sorting algorithm. Gray sub-blocks indicate the main methodological contributions of the proposed method/algorithm to feature extraction (each feature vector (FV) included shape, phase, and distribution features of each spike), *K*-means clustering (with validation indices), and cluster mergence (with clustering evaluation) steps. Notice that, shape features refer to measures extracted from spike waveform in the time domain of the first derivative, phase features refer to measures extracted from spike trajectory in the phase-space (spike first derivative vs. spike second derivative), and distribution features concern to features extracted from spike amplitude distribution function for both the first and second derivatives. At the last step (resulting clusters), a summary sub-block (also in gray) for reporting the relevant information of the whole process was implemented. This approach facilitates the physiological interpretation of the extracted spike features, the assessment of the modulating properties of the involved neurons, and the functional characterization of the neural process under study.

VISSOR Feature Extraction (Figure S2):

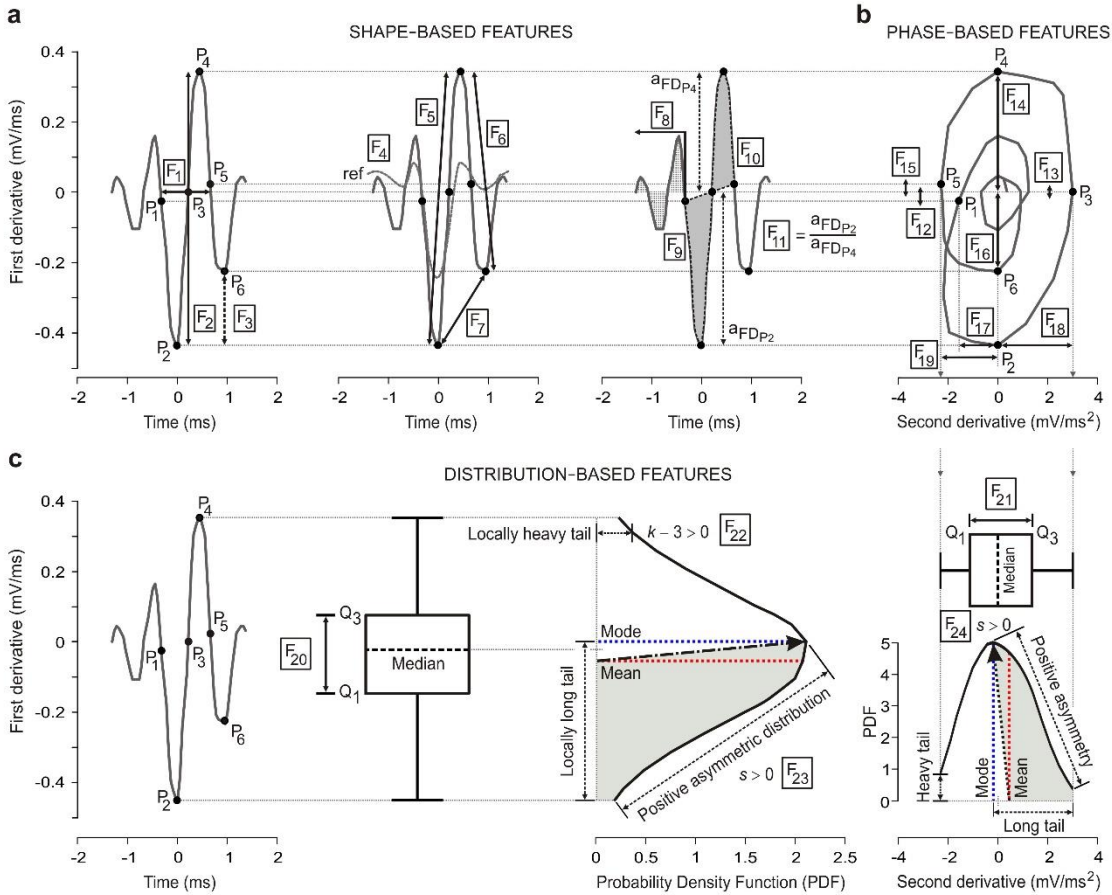


Figure S2. Schematic representation of the feature-extraction method. (a) Six fundamental points ($P_1 - P_6$, see **Table S1** below) and 11 shape-based features ($F_1 - F_{11}$) from each spike event in the time domain of the spike first derivative (FD). (b) Eight phase-based features ($F_{12} - F_{19}$) from each spike trajectory in the phase space (second derivative (SD) vs. FD). (c) Five distribution-based features ($F_{20} - F_{24}$) for the statistical amplitude distribution of the FD (i.e., F_{20} , F_{22} , and F_{23}) and SD (i.e., F_{21} and F_{24}) of the spike. Note that for each spike amplitude distribution (probability density function, PDF), the mean, median, mode, interquartile range ($Q_3 - Q_1$), kurtosis (e.g., $k - 3 > 0$), and asymmetry (e.g., $s > 0$) are indicated. In summary, a vector of 24 features ($F_1 - F_{24}$, see **Table S2** below) was determined for each spike event.

VISSOR Feature Extraction (Tables S1 and S2):

Table S1. List of the selected waveform components. Six fundamental points ($P_1 - P_6$) determined each detected spike. These points were graphically identified in both time domain [see panel (a) in **Figure S2**] and phase space [see panel (b) in **Figure S2**], considering the first derivative (FD) and the second derivative (SD) of the action potential.

Spike-points number	Definition
P_1	First zero-crossing of the FD before the action potential has been detected
P_2	Valley of the FD of the action potential
P_3	Second zero-crossing of the FD of the action potential that has been detected
P_4	Peak of the FD of the action potential
P_5	Third zero-crossing of the FD after the action potential has been detected
P_6	Valley of the FD after the action potential

Table S2. Neurophysiological features of each spike characterizing the process of creating objects (24D feature-vectors). List of shape ($F_1 - F_{11}$), phase ($F_{12} - F_{19}$), and distribution ($F_{20} - F_{24}$) features and their algebraic definition (see **Figure S2**), considering the first derivative (FD) and the second derivative (SD) of each action potential. * The three common features (F_{14} , F_{18} and F_{19}) proposed also by other authors.

	Number	Name	Algebraic definition
SHAPE	F_1	Waveform duration of the FD of the action potential	$t_{P5} - t_{P1}$
	F_2	Peak-to-valley amplitude of the FD of the action potential	$a_{FD_{P4}} - a_{FD_{P2}}$
	F_3	Valley-to-valley amplitude of the FD of the action potential	$a_{FD_{P6}} - a_{FD_{P2}}$
	F_4	Correlation coefficient between the FD of the action potential (ap) and the reference spike-waveform (ref), considering their corresponding standard deviation σ_{FD}	$\frac{\sigma_{FD_{ap,ref}}^2}{\sigma_{FD_{ap}} \cdot \sigma_{FD_{ref}}}$
	F_5	Logarithm of the positive deflection of the FD of the action potential	$\log\left(\frac{a_{FD_{P4}} - a_{FD_{P2}}}{t_{P4} - t_{P2}}\right)$
	F_6	Negative deflection of the FD of the action potential	$\frac{a_{FD_{P6}} - a_{FD_{P4}}}{t_{P6} - t_{P4}}$
	F_7	Logarithm of the slope among valleys of the FD of the action potential	$\log\left(\frac{a_{FD_{P6}} - a_{FD_{P2}}}{t_{P6} - t_{P2}}\right)$
	F_8	Root-mean-square of pre-event amplitudes of the FD of the action potential	$\sqrt{\frac{a_{FD_{P1}} + \sum_{i=m-1}^1 a_i}{m}}$
	F_9	Negative slope ratio of the FD of the action potential	$\left(\frac{a_{FD_{P2}} - a_{FD_{P1}}}{t_{P2} - t_{P1}}\right) / \left(\frac{a_{FD_{P3}} - a_{FD_{P2}}}{t_{P3} - t_{P2}}\right)$
	F_{10}	Positive slope ratio of the FD of the action potential	$\left(\frac{a_{FD_{P4}} - a_{FD_{P3}}}{t_{P4} - t_{P3}}\right) / \left(\frac{a_{FD_{P5}} - a_{FD_{P4}}}{t_{P5} - t_{P4}}\right)$
	F_{11}	Peak-to-valley ratio of the FD of the action potential	$\frac{a_{FD_{P2}}}{a_{FD_{P4}}}$
PHASE	F_{12}	Amplitude of the FD of the action potential relating to P_1	$a_{FD_{P1}}$
	F_{13}	Amplitude of the FD of the action potential relating to P_3	$a_{FD_{P3}}$
	F_{14}^*	Amplitude of the FD of the action potential relating to P_4	$a_{FD_{P4}}$
	F_{15}	Amplitude of the FD of the action potential relating to P_5	$a_{FD_{P5}}$
	F_{16}	Amplitude of the FD of the action potential relating to P_6	$a_{FD_{P6}}$
	F_{17}	Amplitude of the SD of the action potential relating to P_1	$a_{SD_{P1}}$
	F_{18}^*	Amplitude of the SD of the action potential relating to P_3	$a_{SD_{P3}}$
	F_{19}^*	Amplitude of the SD of the action potential relative to P_5	$a_{SD_{P5}}$
DISTRIBUTION	F_{20}	Inter-quartile range ($Q_3 - Q_1$) of the FD of the action potential, considering the percentiles $P_{75_{FD}}$ and $P_{25_{FD}}$	$P_{75_{FD}} - P_{25_{FD}}$
	F_{21}	Inter-quartile range ($Q_3 - Q_1$) of the SD of the action potential, considering the percentiles $P_{75_{SD}}$ and $P_{25_{SD}}$	$P_{75_{SD}} - P_{25_{SD}}$
	F_{22}	Kurtosis coefficient of the FD of the action potential, considering the fourth sampling moment of n amplitudes a_{FD_i} about its mean $\overline{a_{FD}}$, and the standard deviation σ_{FD}	$\frac{\sum_{i=1}^n (a_{FD_i} - \overline{a_{FD}})^4}{n \cdot \sigma_{FD}^4}$
	F_{23}	Fisher asymmetry of the FD of the action potential, considering the third sampling moment of n amplitudes a_{FD_i} about its mean $\overline{a_{FD}}$, and the standard deviation σ_{FD}	$\frac{\sum_{i=1}^n (a_{FD_i} - \overline{a_{FD}})^3}{n \cdot \sigma_{FD}^3}$
	F_{24}	Fisher asymmetry of the SD of the action potential, considering the third sampling moment of n amplitudes a_{SD_i} about its mean $\overline{a_{SD}}$, and the standard deviation σ_{SD}	$\frac{\sum_{i=1}^n (a_{SD_i} - \overline{a_{SD}})^3}{n \cdot \sigma_{SD}^3}$